Technical Report ARWEC-TR-97009

EXPLOSIVE THRUSTER FOR THE ENHANCED ACCURACY KINETIC ENERGY (EAKE) PROJECTILE

Vladimir M. Gold
Brian Fuchs

August 1997

US ARMY
TANK AUTOMOTIVE AND
ARMAMENTS COMMAND
ARMAMENT RDE CENTER

U.S. ARMY ARMAMENT RESEARCH, DEVELOPMENT AND ENGINEERING CENTER

Warheads, Energetics & Combat-support Armaments Center

Picatinny Arsenal, New Jersey

The views, opinions, and/or findings contained in this report are those of the authors(s) and should not be construed as an official Department of the Army position, policy, or decision, unless so designated by other documentation.

The citation in this report of the names of commercial firms or commercially available products or services does not constitute official endorsement by or approval of the U.S. Government.

Destroy this report when no longer needed by any method that will prevent disclosure of its contents or reconstruction of the document. Do not return to the originator.

REPORT DOCUMENTATION PAGE

Form Approved
OMB No. 0704-0188

1. AGENCY USE ONLY (Leave Blank)	2. REPORT DATE	3. REPORT TYPE AND DATES COVERED
	August 1997	Interium/Feb 97

4. TITLE AND SUBTITLE
EXPLOSIVE THRUSTER FOR THE ENHANCED ACCURACY KINETIC ENERGY (EAKE) PROJECTILE

5. FUNDING NUMBERS
EAKE PE 622624

6. AUTHOR(S)
Vladimir M. Gold and Brian Fuchs

7. PERFORMING ORGANIZATION NAME(S) AND ADDRESS(ES)

ARDEC, WECAC
Energetics and Warheads Division (AMSTA-AR-WEE-C)
Picatinny Arsenal, NJ 07806-5000

8. PERFORMING ORGANIZATION REPORT NUMBER

9. SPONSORING/MONITORING AGENCY NAME(S) AND ADDRESS(ES)

ARDEC, WECAC
Information Research Center (AMSTA-AR-WEL-TL)
Picatinny Arsenal, NJ 07806-5000

10. SPONSORING/MONITORING AGENCY REPORT NUMBER

Technical Report
ARWEC-TR-97009

11. SUPPLEMENTARY NOTES

12a. DISTRIBUTION/AVAILABILITY STATEMENT

Approved for public release; distribution is unlimited.

12b. DISTRIBUTION CODE

13. ABSTRACT

A first series of experiments with an explosive thruster for the Enhanced Accuracy Kinetic Energy (EAKE) projectile was conducted. The tested thrusters were LX-14 explosive pellets abutted to a 2-in. diameter and 12-in. long steel bar. The tested explosive weights were 10-g, 20-g, 40-g, and 60-g pellets. The resulting bar velocities were measured using x-ray flash radiography. The performance of the explosive pellets tested was compared with analytical predictions based on Gurney approximations. In all experiments, detonation of the explosive pellets resulted in significant damage imparted to the abutting end of the bar. The extent of this damage increased consistently with increases in the explosive pellet weight. The paper presents a comprehensive discussion of the experiments and the resulting data. A number of recommendations for improving the explosive thruster design are suggested and discussed.

14. SUBJECT TERMS
Kinetic energy projectile Explosive thruster

15. NUMBER OF PAGES
19

16. PRICE CODE

17. SECURITY CLASSIFICATION OF REPORT	18. SECURITY CLASSIFICATION OF THIS PAGE	19. SECURITY CLASSIFICATION OF ABSTRACT	20. LIMITATION OF ABSTRACT
UNCLASSIFIED	UNCLASSIFIED	UNCLASSIFIED	SAR

NSN 7540-01-280-5500

Standard Form 298 (Rev 2-89)
Prescribed by ANSI Std Z39-18
298-102

ACKNOWLEDGMENTS

The authors acknowledge the support of Michael Natalicchio of AMSTA-AR-CCH-A in making this work possible and Brian Travers of AMSTA-AR-WEE-B for manufacturing explosive pellets.

CONTENTS

FIGURES

TABLES

INTRODUCTION

A fin stabilized kinetic energy (KE) projectile entering the air stream with an angle of attack is subject to an "aerodynamic jump," i.e., fast change in projectile Eulerian angles induced from the lift force. According to the Enhanced Accuracy Kinetic Energy (EAKE) projectile concept, the aerodynamic jump can be canceled out by firing an axial thruster located in the fin section of the projectile. Following this concept, the accuracy and the first round hit probability of the KE round can be substantially improved if the corrective impulse is delivered at the proper time (i.e., at the second peak of first yaw cycle) and in the possibly shortest time frame. Delivering the corrective impulse can be accomplished by employing a number of fast reacting energetic materials including: (1) large grain propellants or (2) explosives. The present work follows the latter approach and exploits the feasibility of an explosive thruster charge located in the fin section of the projectile. The principle technical challenge associated with this approach concerns the possible damage to the projectile's fin section resulting from detonating the explosive. Therefore, the working rationale for designing the explosive thruster is that the blast resulting from detonating the explosive has to supply the required impulse, but must not compromise the structural integrity of the projectile's fin section. The present work is concerned with the first step in designing the thruster charge, i.e., to determine the weight of the explosive that is necessary for delivering the axial impulse required.

EXPERIMENTS

In order to minimize the experimental costs, the KE projectile was simulated with a 2-in. diameter and 12-in. long circular cylindrical bar of the same mass (≈5 kg). All steel bars employed in the experiments were manufactured from AISI 4340 steel. The machined bars were heat treated at 1090°K for 2 hrs, followed by quenching in an oil bath. Heat treatment resulted in an average hardness of 40 R_C.

The design of the experimental explosive thrusters tested is shown in figure 1. The thruster consisted of a truncated cone pellet of high explosive positioned flush at the end of the bar. Because the precision in positioning the explosive pellet (with respect to the axis of steel bar) significantly effects the direction of the delivered impulse (which is crucial for proper functioning the thruster), the pellets were centered using plastic pellet holders (fig. 1).

A total of 10 explosive pellets were tested: three 10-g pellets, three 20-g pellets, two 40-g, and two 60-g pellets. All explosive pellets were manufactured from (either 1.5-in. diameter and 1-in. long or 3.5-in. diameter and 7-in. long) billets of LX-14 explosive pressed to an average density of 1.81 g/cm^3. The explosive pellets were initiated using RP-501 EBW detonators (containing 136 mg of PETN explosive) and auxiliary 2.7-g explosive boosters. All boosters pellets were 0.5-in. diameter and 0.5-in. long circular

cylinders manufactured from PBXN-5 (95% of HMX and 5% Viton A) explosive. The pellet holders were manufactured from LEXAN™* (polycarbonate) plastic. The detonator holders were manufactured from aluminum. The details of the design of explosive pellets, the explosive boosters, the explosive pellet holders and the detonator holders including all relevant dimensions, are given in figure 1. All parts were manufactured with a tolerance of 0.005 in. Because of the explosive safety considerations, the explosive thrusters were assembled only prior to testing. The experiments were conducted at the Picatinny Arsenal Small Scale Explosive Experimental Site.

The schematic of the experimental setup is shown in figure 2. Steel bars (simulating KE projectiles) were freely suspended from the experimental chamber ceiling using a pair of 0.07-in. diameter cotton strings. At the ceiling, the strings were attached to two eye-bars approximately 13 in. apart each from the other. At the opposing ends (approximately 96 in. down from the ceiling), the strings were tied up near the ends of the bar. The 0.07-in. diameter strings had sufficient strength to support the bar's weight only prior to detonating the explosive. A short time following the explosion, the supporting strings break and the bar is free in the air; a situation which is similar to the conditions of a KE projectile flying in a free air.

The experimental arrangement employed was designed assuming that the thruster propels the bar strictly in the axial direction (the objective of the thruster is to deliver an explosive impulse only in the axial direction). However, as discussed, the bar is not restrained and it is free to move in any direction. Therefore, any motion of the bar other than the axial translation can introduce significant errors in measuring the total explosive impulse delivered. The possible modes of the motion of the bar are as follows:

- Under the gravitational force, the bar is free to translate vertically. The bar's vertical displacement, due to gravitational acceleration, is $\Delta=(gt^2)/2$. Assuming that the time frame of a typical experiment $t<10$ ms, the resulting vertical displacement is $\Delta\approx5\cdot10^{-4}$cm. This is negligible in comparison to the bar's axial displacement $\Delta_Z=\mu\cdot(\Delta_F-\Delta_0)$ due to the explosive impulse, which was in the order of 1 to 4 cm (table 1).

- A string suspended bar is free to rotate. Therefore, some rotational motion may occur also, primarily due to a possible misalignment between axis of the explosive pellet and the bar. Post-test analysis of flash radiographic images of the moving bar did not show presence of any significant rotational motion. This proved our original caution in manufacturing and assembling all parts of the thruster with the highest precision possible.

*Lexan is the trade mark for

The employed flash radiographic system consisted of two separate x-ray tubes **A** and **B** (fig. 2), which were triggered sequentially at given times t_A and t_B, respectively. Exposing the moving bar twice creates two separate images, which are superimposed on the same film [e.g., test 4-439 (fig. 3)]. Referring to figure 3, the axial offset between two superimposed images represents the axial displacement Δ_f of the bar within the time between exposures at t_A and t_B. Because the axis of the tubes **A** and **B** are at an angle, a static offset between the images Δ_0 has to be accounted for by subtracting Δ_0 from the displacement Δ_f. Thus, the velocity of the bar can be computed as $V=\mu\cdot(\Delta_f-\Delta_0)/(t_A-t_B)$, where μ is a given x-ray magnification factor. The resulting x-ray film data is summarized in table 2.

Since measuring the resulting bar velocity was one of the principal objectives of this series of experiments, the flash radiographic system was backed up with an auxiliary (break gauge) velocity measurement system shown in figure 4. The employed gauges were constructed using acrylic frames, which held a total of three break wires, evenly spaced with a distance of 0.5 in. apart. The first wire was positioned at a distance S=2 in. in the front of the bar (fig. 2). Initially, the gauges were constructed using 0.004-in. copper wires, with strength low enough to be easily broken by a moving bar. Post-test analysis of break wire trigger times showed massive discrepancies in all data collected, including the data from the adjacent wires, as well as the data resulting from different experiments. This suggested a hypothesis that the wires were triggered by a mechanism different than the intended, most likely by the air shock resulting from the explosion. Increasing the thickness of the wires to 0.010 in. was to no avail.

The latter hypothesis can be supported by the following analysis. The time required for the air shock to reach the first wire is $t_{air}=P/c_{air}$, where c_{air} is the air sound speed ($c_{air}\approx$300 m/s) and P is the length of the shortest path from the explosive pellet to the first wire, $P\approx L+S$=14 in. (L=12 in. is the length of the bar). Thus, $t_{air}\approx$1.2 ms. In the case when the wires are triggered by a moving bar and not by the air shock, the time at which the first wire is broken can be calculated as follows: assume that the bar reaches final velocity (V) with a third elastic wave reflection (off the free end), i.e., at time $\tau=5L/c_s$, where c_s is the sound speed in steel ($c_s\approx$5,000 m/s). This results in $\tau\approx$0.31 ms. The highest velocity achieved in the experiments was V=20 m/s (table 1). Thus, assuming that the bar was accelerated to this velocity through a series of linearly increasing steps, the first wire trigger time is $t_{bar}=\tau+(S-\frac{1}{2}\cdot V\cdot\tau)/V=\frac{1}{2}\cdot\tau+S/V$, resulting in $t_{bar}\approx$2.75 ms. Since this value is more than twice the value of the time required for the air shock to reach the break gauge system, it is most likely that the wires were triggered due to the air shock, and not due to the motion of the bar.

Soft recovery boxes were constructed from wood and construction foam. Albeit that in all tests the bars bounced out of the recovery boxes, the employed catch boxes were found to be quite adequate for recovering the bars without any additional damage (which was limited only to minor scratches and tiny dents). In all experiments, the detonation of the explosive pellets resulted in a significant damage imparted to the abutting end of the bar.

The extent of this damage increased consistently with increases of the explosive pellet weight. A post-test photograph comparing all tested bars is shown in figure 4. As shown in figure 4, the fracturing observed was well repeatable from an experiment to an experiment. The experiments with 10-g and 20-g pellets resulted only in moderate damage to the abutting bar end. In these cases, the damage was confined to a central well rounded shallow dent, surrounded by a circular zone of partially fractured material. In the case of 10-g pellets, the size of the dent was approximately 3 cm in diameter; in the case of 20-g pellets the size of the dent was approximately 3.7 cm in diameter. In the case of 10-g pellets, the dent was surrounded by a narrow, but quite discernible circumferential fissure. In the case of 20-g pellets, the zone surrounding the dent failed, apparently in brittle fracture. In some of the experiments, thin irregular radial cracks were also present, predominately in the dented area. In the case of both the 40-g pellets and the 60-g pellets, the material at the lateral boundary fractured completely, only the central core remained intact. The diameter of this core decreased with increases in the pellet size: for 40-g pellets the average core diameter was approximately 1.0 cm; however, for 60-g pellets, only 0.5 cm of the core remained. In both these cases, the length of the fracture zone was approximately 4.0 to 6.0 cm. Since all bars tested were heat hardened, the failed bar's material exhibited distinct features of tensile brittle fracture (i.e., characteristically rugged and grainy grayish failure surfaces), apparently due to strong tensile stress waves.

The physics of the tensile fracture of the bar's end abutted to the explosive is as follows: referring to figure 5, detonating the explosive generates a shock wave which propagates into the bar with velocity u_s. As the shock wave pulse progresses axially into the bar, a dilatational (or rarefaction) wave follows behind it, originating at the lateral surface. This process continues until the tensile wave eventually catches up with the shock. Behind the shock wave, the material is compressed to pressure p. The magnitude of this pressure is a function of the detonation properties of the explosive and the shock properties (Hugoniot) of the bar's material. Generally, for a fixed explosive type, the higher the density of the material abutting the explosive is, the higher the resulting pressure p, a consideration which may be useful for maximizing the explosive impulse delivered without damaging the bar. For example, in the case of steel, $p \approx 0.55$ Mbar, while for the titanium, the pressure transmitted to the bar is significantly lower, only approximately 0.4 Mbar. The lateral boundary of the bar is at ambient atmospheric pressure $p_0 \approx 1$ Bar, and the bar's material is free to expand radially. This generates a cylindrical dilatational wave originating at the bar's surface and propagating towards the bar's axis with a velocity u_r.

Behind the front of the dilatational wave, the bar's material is in tension, while ahead of the wave front the bar's material is in compression. The instantaneous radial stress profile along the radial direction is as follows: at the bar's surface the stress is zero (or, rather, 1 Bar); towards the center the stress is continuously increased, reaching its maximum at the front of the wave. As the dilatational wave progresses towards the center, the radial stress component (which must balance the radial momentum of the dilated material) increases until the tensile strength limit is reached. At this point, the bar may fracture radially. As the dilated portion of the bar continues to expand radially, the circumferential

component of the stress may exceed the tensile strength, which may lead to multiple radial cracks and fractures. As the shock wave pulse progresses axially into the bar, the rarefaction wave follows behind it, which continues until the tensile wave eventually catches up with the shock. The time when the rarefaction wave reaches the shock wave front marks the end of the possible fracture zone, which is a strong function of the geometry of the bar and the pellet, as well as the shock properties of the bar's material. This is the reason why in the case of both the 40-g and the 60-g pellets (which both had similar diameters: 4.4 cm and 5.1 cm, respectively), the length of the fracture zone was approximately the same, regardless of the explosive pellet weight.

Figure 6 is a summary of results of this series of experiments. The solid line appearing in this figure refers to analytical predictions based on Gurney approximations (for an "open-face sandwich" type configuration). Since in the Gurney analysis the geometry is planar with no losses at the charge boundary, the solid line represents the "upper limit" of the performance expected, provided that the explosive charge is not confined from the back (i.e., open-face sandwich type configuration). As shown in figure 6, the performance of the tested pellets is significantly below this upper limit, especially in the case of the higher explosive weights. The observed decrease in the performance is due to energy losses at the charge boundary. As shown in figure 6, in order to achieve the corrective impulse required (I=11.12 g· cm/μs), it behooves that about 75 g of the explosive, which is approximately 40% higher than the weight based on the Gurney approximation (45 g).

The recommendations for improving the explosive thruster design are as follows:

- The experiments showed that employing pellet weights exceeding 40 g of explosive resulted in almost complete fragmentation of the abutted end of the bar, mostly because of the low tensile strength of the heat hardened steel used. Employing AISI 4340 steel with a different heat treating process may significantly reduce overall damage imparted into the bar. The working rationale for designing the thruster is to maximize the delivered impulse without compromising the structural integrity of the projectile's fin section. Therefore, the next design iteration should concentrate on improvements aimed to minimize the damage imparted to the bar, rather than to maximize the efficiency of the explosive energy transfer. To reduce the projectile's end shatter, all possible techniques should be considered and explored. At this point, the following thruster design modification can be suggested: (1) introduction of a shock pressure reducing buffer (between the explosive and the bar) combined with (2) limited design modifications to the projectile's fin section.

- The magnitude of the axial impulse delivered can always be adjusted by increasing the explosive pellet weight, provided that the structural integrity of the projectile's fin section is not compromised. Once such a "robust"

design is established, the thruster performance can be enhanced by maximizing its efficiency in transferring the momentum from explosive pellet to the projectile. In general, this can be achieved by minimizing side losses at the pellet boundary. At this point, only a limited number of possible design improvements may be suggested: heavy confinement of the explosive pellet (which is also beneficial for protecting the explosive from high pressures and temperatures due to the burning of the surrounding propellant) and some refinements in the overall pellet's geometry, *etc.*

CONCLUSIONS

A series of experiments with LX-14 Explosive Thrusters abutted to 5-kg steel bars has been conducted. The tested explosive pellet weights were 10-g, 20-g, 40-g, and 60-g pellets. The corresponding bar velocities were in the range between 4 m/s to 20 m/s and increased approximately linearly with increases in the pellet weights. Analysis of the obtained (velocity versus the explosive charge weight) data showed that increasing the explosive pellet size degraded the efficiency of the explosive, apparently due to the relatively higher energy losses at the pellet boundary. Extrapolating the resulting data to achieve the axial thrust of I=11.12 g· cm/μs, should require approximately 75 g of explosive. However, the experiments show that blasting as low as 40 g of the explosive is capable of partially shattering the abutted end of the bar. Thus, the tested explosive thruster can not deliver the required corrective impulse without compromising the structural integrity of the projectile's fin section. To achieve the desired design objective requires significant modifications to the design tested, which needs extensive numerical simulations and further experimentation.

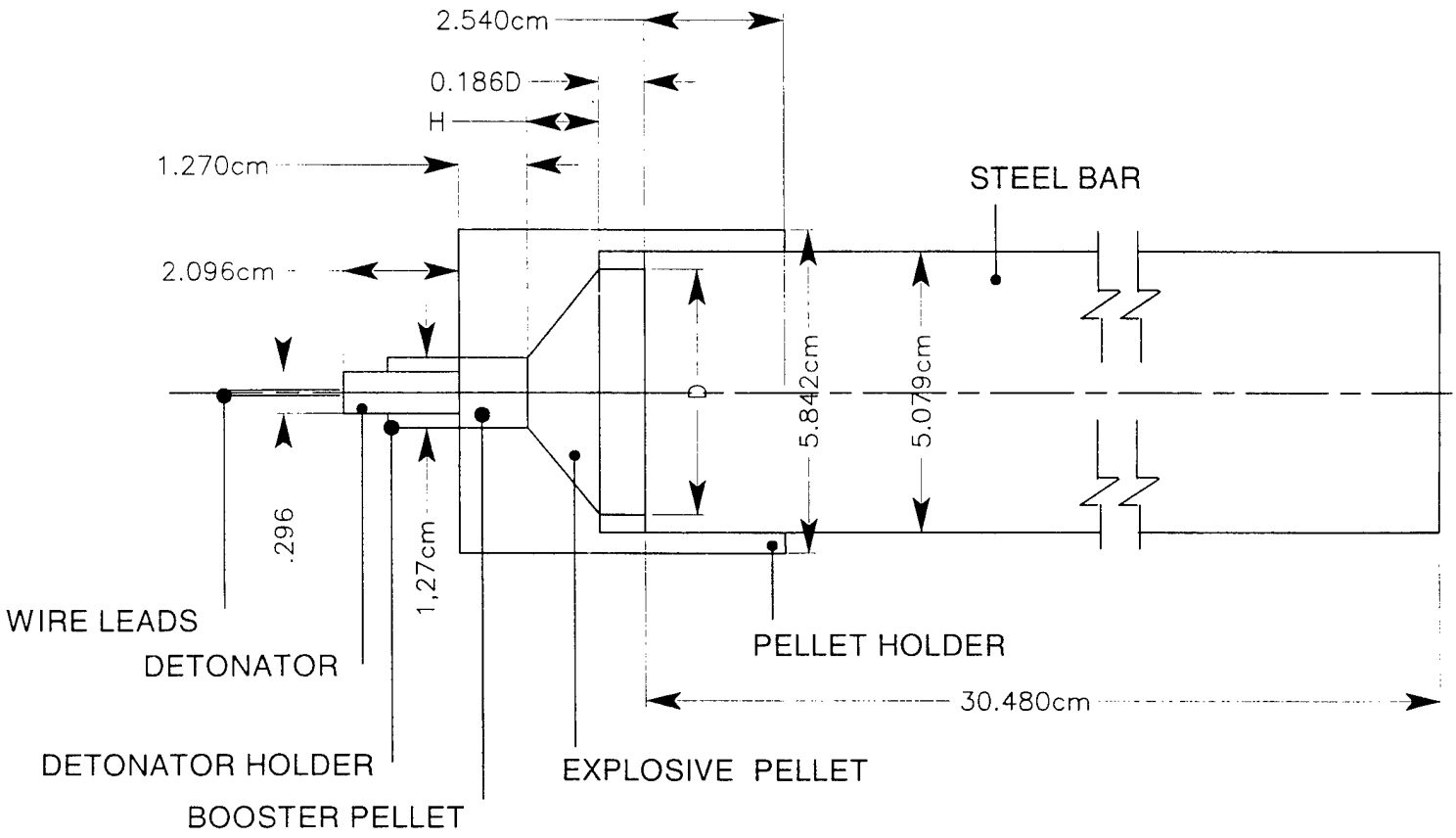

Pellet Weight W, g	Pellet Diameter D, cm	Pellet Height H, cm
10	2.745	0.248
20	3.521	0.367
40	4.437	0.516
60	5.079	0.621

Figure 1
Simulant projectile and the explosive thruster assembly

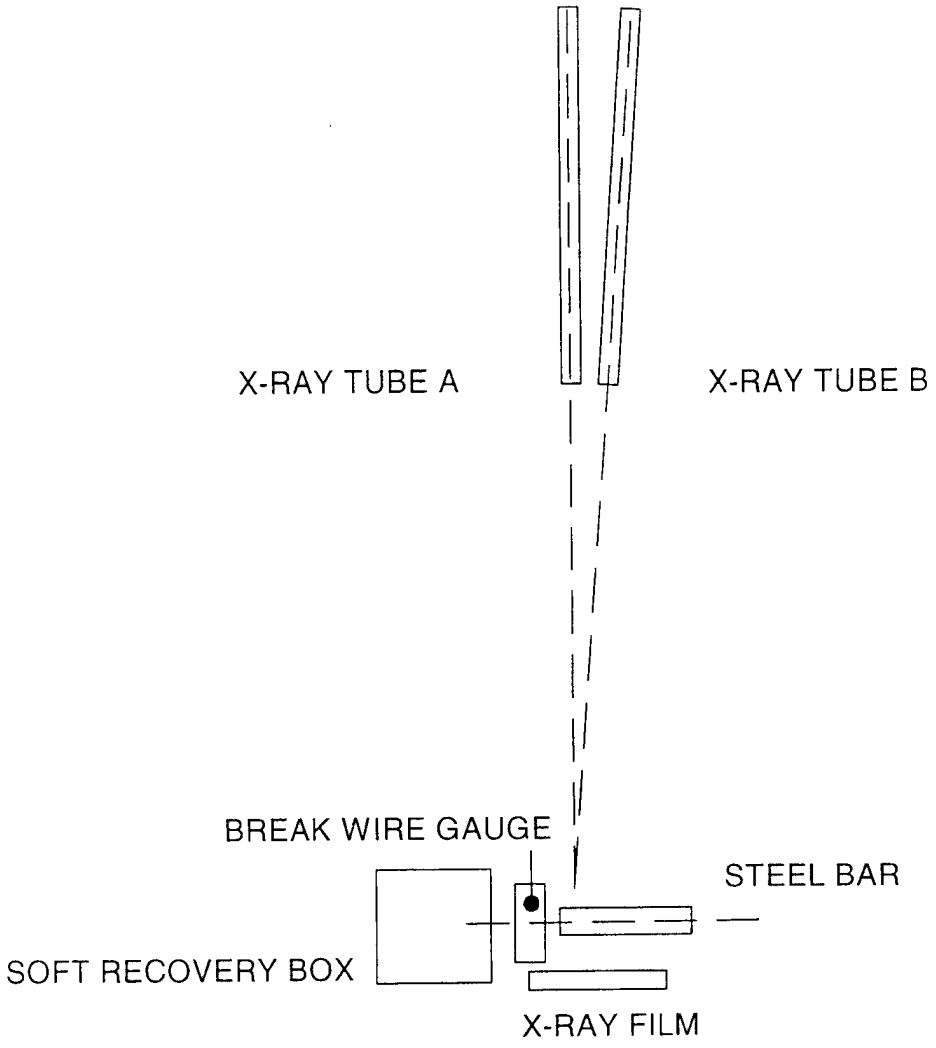

Figure 2
Experimental setup

Figure 3
Flash radiograph of moving bar

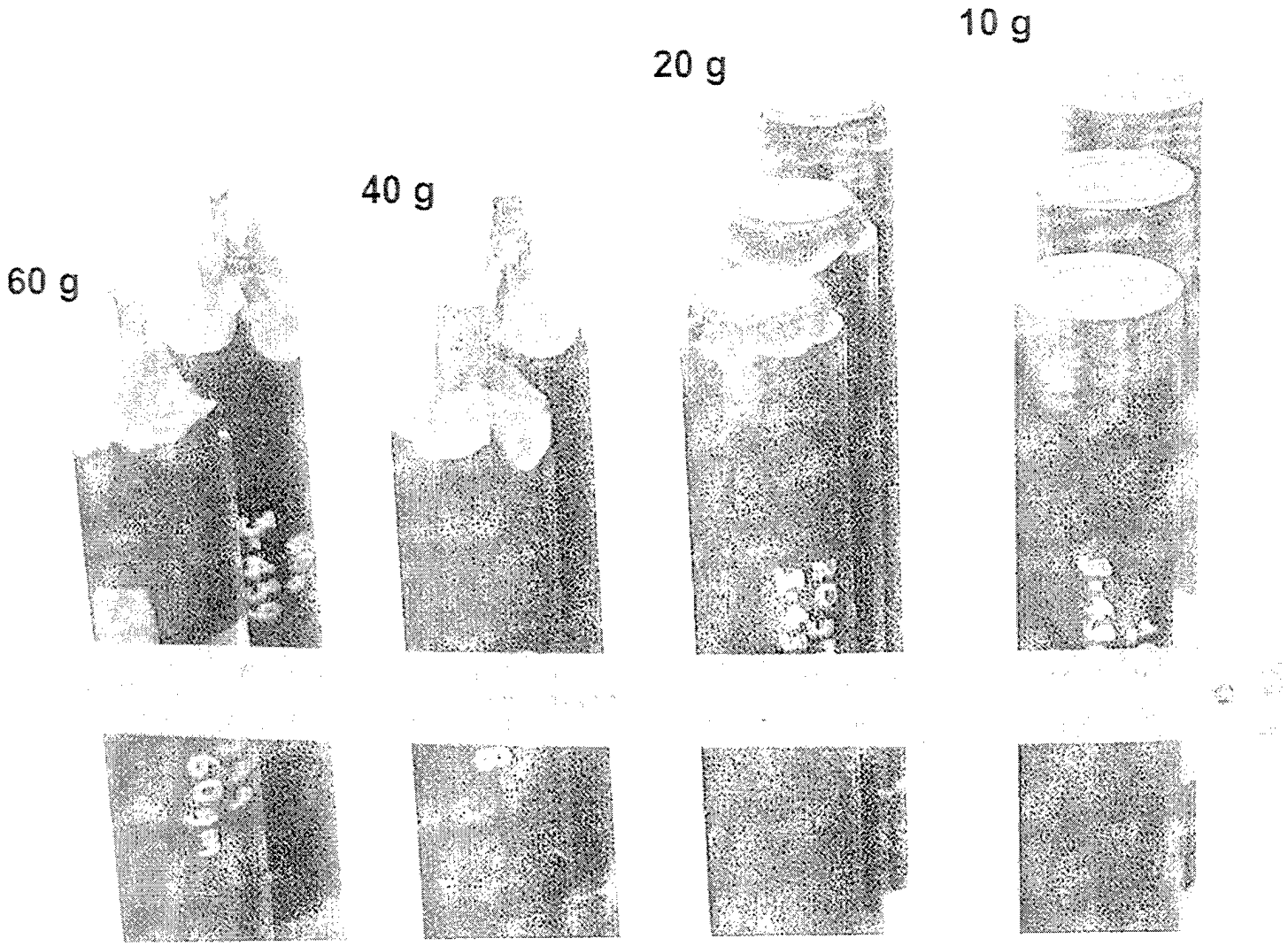

Figure 4
Post-test photograph of the steel bars

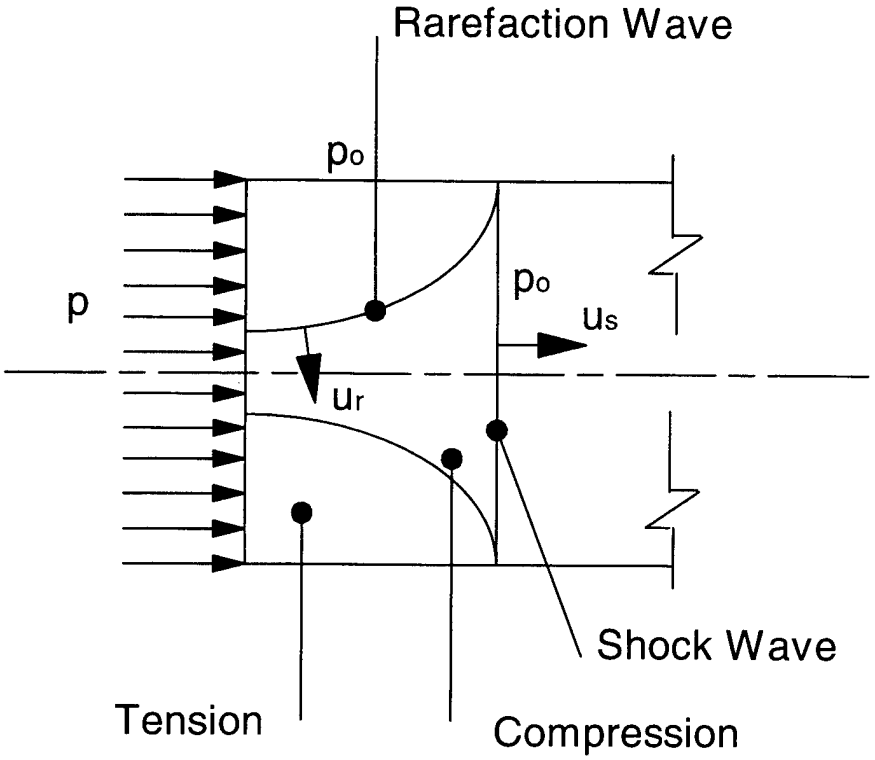

Figure 5
Propagation of shock and dilatational waves following explosion

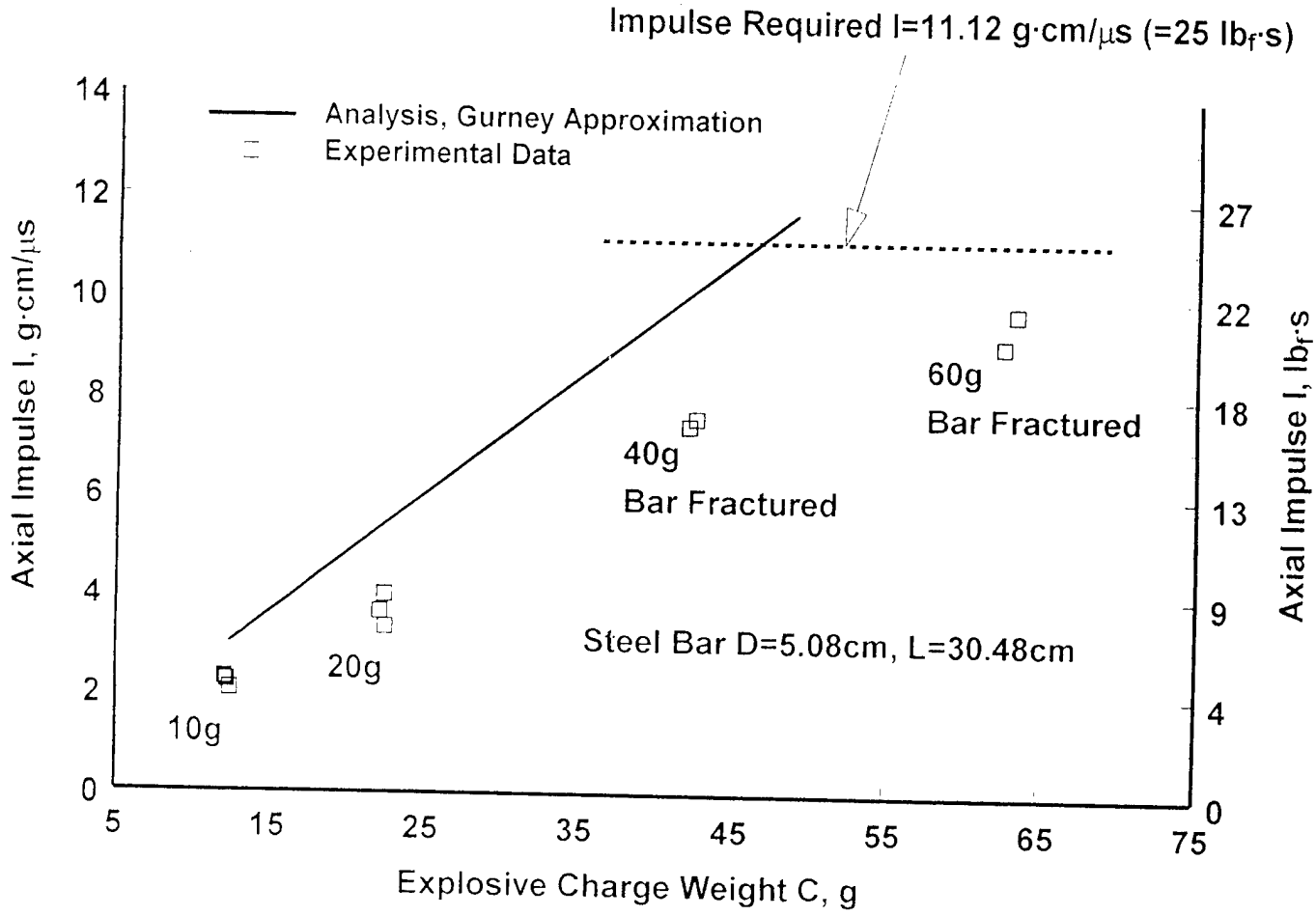

Figure 6
Axial impulse versus the explosive charge weight

Table 1
Summary of the experimental data

Test no.	Explosive pellet nominal weight (g)	Explosive pellet and booster weight *C*, g	Bar mass *M*, g	Velocity *V*, m/s
3-436	10	12.50	4,789	4.27
3-437	20	22.60	4,802	6.90
3-438	40	42.15	4,815	15.35
3-439	60	63.38	4,802	20.26
3-440	10	12.50	4,795	4.74
3-441	20	22.26	4,788	7.58
3-442	40	42.59	4,795	15.75
3-443	10	12.29	4,782	4.64
3-444	60	62.59	4,891	18.56
3-445	20	22.54	4,796	8.27

Table 2
Flash radiographic data

Test no.	X-ray magnification factor (μ)	Static offset Δ_0, mm	Dynamic axial displacement Δ_f, mm	Tube A flash time t_A, ms	Tube B flash time t_B, ms
3-436	0.95019	7.491	18.895	5.082	2.542
3-437	0.95023	7.950	26.383	5.082	2.543
3-438	0.95016	7.405	27.932	2.542	1.271
3-439	0.95012	7.128	25.171	1.694	0.848
3-440	0.95016	7.016	32.328	10.160	5.082
3-441	0.95016	5.233	45.747	10.160	5.082
3-442	0.95016	7.561	26.122	0.5094	2.541
3-443	0.95016	7.304	15.582	3.389	1.695
3-444	0.95016	7.356	40.439	3.390	1.695
3-445	0.96008	6.763	40.023	7.621	3.382

DISTRIBUTION LIST

Commander
Armament Research, Development and Engineering Center
U.S. Army Tank-automotive and Armaments Command
ATTN: AMSTA-AR-WEL-TL (2)
AMSTA-AR-GCL
AMSTA-AR-CCH-A (2)
AMSTA-AR-FST-T
AMSTA-AR-WEE
AMSTA-AR-WEE-C, Dr. V. Gold (5)
Picatinny Arsenal, NJ 07806-5000

Defense Technical Information Center (DTIC)
ATTN: Accession Division (12)
8725 John J. Kingman Road, Suite 0944
Fort Belvoir, VA 22060-6218

Director
U.S. Army Materiel Systems Analysis Activity
ATTN: AMXSY-EI
392 Hopkins Road
Aberdeen Proving Ground, MD 21010-5423

Commander
Chemical/Biological Defense Agency
U.S. Army Armament, Munitions and Chemical Command
ATTN: AMSCB-CII, Library
Aberdeen Proving Ground, MD 21010-5423

Director
U.S. Army Edgewood Research, Development and Engineering Center
ATTN: SCBRD-RTB (Aerodynamics Technology Team)
Aberdeen Proving Ground, MD 21010-5423

Director
U.S. Army Research Laboratory
ATTN: AMSRL-OP-CI-B, Technical Library
Aberdeen Proving Ground, MD 21005-5066

Chief
Benet Weapons Laboratory, CCAC
Armament Research, Development and Engineering Center
U.S. Army Tank-automotive and Armaments Command
ATTN: AMSTA-AR-CCB-TL
Watervliet, NY 12189-5000

Director
U.S. Army TRADOC Analysis Command - WSMR
ATTN: ATRC-WSS-R
White Sands Missile Range, NM 88002

Commander
Naval Air Warfare Center Weapons Division
1 Administration Circle
ATTN: Code 473C1D, Carolyn Dettling (2)
China Lake, CA 93555-6001

GIDEP Operations Center
P.O. Box 8000
Corona, VA 91718-8000

Department of Civil and Environmental Engineering
Penn State University
ATTN: Professor T. Krauthammer
212 Sackett Building
University Park, PA 16802-1408